Potential Design for Electron Transmission in Semiconductor Devices

Jun Zhang, *Senior Member, IEEE*, and Robert Kosut, *Fellow, IEEE*

***Abstract*—In this brief, we discuss the design of electrostatic potential profile to achieve a desired electron transmission coefficient versus bias voltage characteristics in nanoscale semiconductor devices. This is a common problem in the design of many new electronic devices. We formulate it as a constrained optimization problem, and solve it by sequential linear programming. We further investigate the robust design of potential that is tolerant to noise, disturbance, and parameter uncertainty in the device.**

***Index Terms*—Electron transmission, minimax, potential profile, robust optimal design, sequential linear programming.**

I. Introduction

With the rapid development of sophisticated fabrication techniques, it has recently become possible to create nanoscale semiconductor devices with dimensions at several nanometers. Examples of such devices include quantum dots [1], nanowires [2], and electron gas in GaAs-AlGaAs heterostructures [3]. For semiconductor devices of this size, many quantum mechanical effects can be observed such as tunneling and nonequilibrium behaviors. Such effects are critical in the design of many new electronic devices such as nanoscale transistors (see, e.g., [4]).

The objective of this brief is to design an electrostatic potential profile for electron transmission in a prototype nanoscale semiconductor device. We assume that the barrier layers of this nanodevice have fixed width and can be grown to obtain an accurate potential. For an electron at a given energy transporting through such a device, its transmission coefficient can be described as a function of both the local potential and externally applied bias voltage. We want to design a local potential to achieve a prescribed transmission coefficient versus bias voltage characteristics, e.g., a linear or quadratic function.

The potential design in semiconductor devices to achieve desired transmissions has been previously addressed in [5] and [6]. Exhaustive numerical search was used in [5] to find solutions. This takes enormous computing time and thus is infeasible in the real design practice. In [6], an adjoint method was developed to efficiently and accurately compute gradients for the optimal design of electronic devices. The numerical stability and convergence of the state equations and their gradients were rigorously established.

In this brief we develop a sequential linear programming algorithm to solve the potential design problem. Different from [6], we focus on the development of optimization algorithms and also the robust optimal design tolerant to parameter uncertainties. In the case when there is no uncertainty, we transform it into a minimax problem by evaluating the maximum error between the desired and the actually achieved transmission-voltage characteristics. From first order approximation, we obtain a sequential linear programming problem. The significance of this approach is that it deals with constraints in a straightforward manner. Moreover, in each iteration we need only to handle a linear programming problem, which can be solved efficiently by mature numerical procedures.

To solve the Schrödinger equation that determines the wave function of an electron, we use the state transition matrix approach. The main advantage is that we can analytically calculate the derivative of the transmission coefficient with respect to the potential profile. This leads to the direct computation of gradient and thus facilitates the applications of local optimization algorithms.

Furthermore, we investigate the robust potential design. In the real physical implementations, it is inevitable that there exist various noise, disturbance, and parameter uncertainty in the device. We aim at designing potential that is robust against these adverse effects, i.e., it should provide uniform transmission characteristics even if the actual system implemented differs from the nominal model used for design. Such robust design is particularly important in the real engineering of semiconductor devices. We use a Monte Carlo-based optimization procedure by generating a large number of samples which numerically characterize the statistics of the parameter uncertainty, and then engage sequential quadratic programming to find the robust design. The resulting potential profile is shown to have better robust performance.

II. Problem Statement

Restricting attention to a single spatial dimension, we consider an electron transporting through a prototype nanoscale semiconductor device as shown in Fig. 1 [5]. The semiconductor material is sandwiched between n-type electrodes with carrier concentration $N_1 = 10^{24}$ m^{-3}. In the manufacturing process, a local potential U can be accurately produced by growing layers in the range $[0, d_2]$. Assume that there are N layers with equal width $\delta x = d_2/N$ and the local potential in the ith barrier layer is U_n, i.e.,

$$U(x) = U_n, \quad x \in [x_n, x_{n+1}], \quad n = 1, \ldots, N$$

where $x_1 = 0$ and $x_{N+1} = d_2$. Outside the range $[0, d_2]$, assume that the potential is U_0 for $x \leq 0$ and U_{N+1} for $x \geq d_2$.

Manuscript received November 30, 2011; accepted February 01, 2012. Manuscript received in final form February 03, 2012. Date of publication March 14, 2012; date of current version nulldate. The work of J. Zhang was supported by the Innovation Program of Shanghai Municipal Education Commission under Grant 11ZZ20, Shanghai Pujiang Program under Grant 11PJ1405800, NSFC under Grant 61174086, and State Key Lab of Advanced Optical Communication Systems and Networks, SJTU, China. Recommended by Associate Editor A. G. Alleyne.

J. Zhang is with the Joint Institute of UMich-SJTU, Shanghai Jiao Tong University, and Key Laboratory of System Control and Information Processing, Ministry of Education, Shanghai 200240, China (e-mail: zhangjun12@sjtu.edu.cn).

R. Kosut is with SC Solutions Inc., Sunnyvale, CA 94085 USA (e-mail: kosut@scsolutions.com).

Color versions of one or more of the figures in this brief are available online at http://ieeexplore.ieee.org.

Digital Object Identifier 10.1109/TCST.2012.2187337

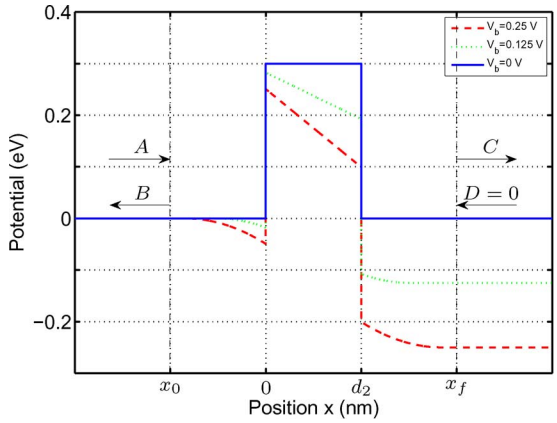

Fig. 1. Potential profiles. Blue solid line: $U(x)$; Green dotted line: total potential $U(x)+\phi(x,V_b)$ when $V_b=0.125$ V; Red dashed line: total potential $U(x)+\phi(x,V_b)$ when $V_b=0.25$ V. Here $\phi(x,V_b)$ are calculated from (2)–(4).

Suppose that an electron is incident from the far left. The electron wave function $\psi(x)$ satisfies the following time independent Schrödinger equation:

$$-\frac{\hbar^2}{2m}\frac{d^2\psi(x)}{dx^2}=(E-\phi(x)-U(x))\,\psi(x) \tag{1}$$

where m is the effective electron mass, E the energy of the incident electron, $U(x)$ the potential profile, and $\phi(x)$ the conduction band potential defined in the region $[x_0,x_f]$.

The conduction band potential $\phi(x)$ is the result of applying a bias voltage V_b to the semiconductor device, and it can be determined by solving Poisson equation [7]. In general $\phi(x)$ and $\psi(x)$ are coupled. Solving Schrödinger and Poisson equations in a self-consistent manner demands tremendous computational resources. For the prototype device discussed here, we assume that the application of bias voltage creates thin enough negative charge accumulation layer on the left side and depletion layer on the right side of the barrier. Therefore, the charge density is 0 in the region $[0,d_2]$ and constants outside this region. Together with appropriate boundary conditions, the conduction band potential can be approximated by a linear function on the barrier layers $[0,d_2]$ and quadratic function outside this interval as follows [5], [6]:

$$\phi(x,V_b)=\begin{cases}0, & \text{if } x\le -d_1\\ -\frac{q}{2\epsilon_1 d_1}(x+d_1)^2, & \text{if } -d_1\le x<0\\ -\frac{qd_1}{2\epsilon_1}-\frac{q}{\epsilon_2}x, & \text{if } 0\le x<d_2\\ -V_b+\frac{q(x-(d_1+d_2))^2}{2\epsilon_1 d_1}, & \text{if } d_2\le x<d_1+d_2\\ -V_b, & \text{if } x\ge d_1+d_2\end{cases} \tag{2}$$

where

$$d_1=-\frac{d_2\epsilon_1}{2\epsilon_2}+\sqrt{\frac{V_b}{\epsilon_1 N_1}+\left(\frac{d_2\epsilon_1}{2\epsilon_2}\right)^2} \tag{3}$$

$$q=\frac{V_b}{d_1/\epsilon_1+d_2/\epsilon_2}. \tag{4}$$

Here ϵ_0 is the permittivity of free space, $\epsilon_1=13.1\epsilon_0$ the dielectric constant of GaAs, and $\epsilon_2=10.1\epsilon_0$ the dielectric constant of AlGaAs. Based on (2)–(4), we plot the total potential $U(x)+\phi(x,V_b)$ for $U(x)=0.3$ V and several different values of V_b in Fig. 1.

Our target is to design a potential profile $U(x)$ so as to achieve a prescribed transmission coefficient T versus bias voltage V_b characteristics. We first introduce a state transition matrix approach to calculate the transmission coefficient $T(V_b)$ for a given bias voltage V_b and a potential $U(x)$.

For the region $x<x_0$ in Fig. 1, where $\phi(x)=0$ and $U(x)=U_0$, the solution of Schrödinger (1) can be written in a general form as

$$\psi(x)=A\exp(ik_0x)+B\exp(-ik_0x) \tag{5}$$

where $k_0=\sqrt{2m(E-U_0)}/\hbar$; and for $x>x_f$, where $\phi(x)=-V_b$ and $U(x)=U_{N+1}$, the solution can be written as

$$\psi(x)=C\exp(ik_fx)+D\exp(-ik_fx) \tag{6}$$

where $k_f=\sqrt{2m(E-U_{N+1}+V_b)}/\hbar$. Here A and C are traveling wave coefficients for the wave functions from left to right, and B and D are the corresponding coefficients from right to left. We set $D=0$ since the electron is assumed to be incident from the left and there is no reflection at the far right. These coefficients are yet to be determined, and we are interested in the transmission coefficient that is defined as $T=|C|^2/|A|^2$ [8].[1] Let $\psi_1(x)=\psi(x)$ and $\psi_2(x)=\dot{\psi}(x)$. We can write Schrödinger equation (1) as a linear vector differential equation

$$\frac{d}{dx}\begin{bmatrix}\psi_1(x)\\ \psi_2(x)\end{bmatrix}=\begin{bmatrix}0 & 1\\ -K(x) & 0\end{bmatrix}\begin{bmatrix}\psi_1(x)\\ \psi_2(x)\end{bmatrix} \tag{7}$$

where $K(x)=2m(E-\phi(x)-U(x))/\hbar^2$. The state transition matrix $\Phi(x,x_0)$ for (7) is defined by

$$\begin{bmatrix}\psi_1(x)\\ \psi_2(x)\end{bmatrix}=\Phi(x,x_0)\begin{bmatrix}\psi_1(x_0)\\ \psi_2(x_0)\end{bmatrix} \tag{8}$$

and it satisfies

$$\frac{d\Phi(x,x_0)}{dx}=\begin{bmatrix}0 & 1\\ -K(x) & 0\end{bmatrix}\Phi(x,x_0),\ \Phi(x_0,x_0)=I_2 \tag{9}$$

where I_2 is the 2×2 identity matrix.

The solutions in (5) and (6) must satisfy the following boundary conditions:

$$\begin{bmatrix}\psi_1(x_0)\\ \psi_2(x_0)\end{bmatrix}=\begin{bmatrix}\exp(ik_0x_0) & \exp(-ik_0x_0)\\ ik_0\exp(ik_0x_0) & -ik_0\exp(-ik_0x_0)\end{bmatrix}\begin{bmatrix}A\\ B\end{bmatrix} \tag{10}$$

and

$$\begin{bmatrix}\psi_1(x_f)\\ \psi_2(x_f)\end{bmatrix}=\begin{bmatrix}1\\ ik_f\end{bmatrix}C\exp(ik_fx_f). \tag{11}$$

From (8), we have

$$\begin{bmatrix}\psi_1(x_0)\\ \psi_2(x_0)\end{bmatrix}=\Phi(x_0,0)\Phi(0,d_2)\Phi(d_2,x_f)\begin{bmatrix}\psi_1(x_f)\\ \psi_2(x_f)\end{bmatrix}. \tag{12}$$

Substituting (10) and (11) into (12), we obtain

$$A=\frac{1}{2}e^{-ik_0x_0}[1\quad -i/k_0]\Phi(x_0,0)\Phi(0,d_2)\times\Phi(d_2,x_f)\begin{bmatrix}1\\ ik_f\end{bmatrix}Ce^{ik_fx_f}$$

[1]Note that the definition we adopt here differs slightly from the definition in, e.g., [9].

and the transmission coefficient then becomes

$$T = \frac{|C|^2}{|A|^2} = \frac{4}{\left|[1 \quad -i/k_0]\Phi(x_0,0)\Phi(0,d_2)\Phi(d_2,x_f)\begin{bmatrix}1\\ik_f\end{bmatrix}\right|^2}.$$

Note that $\Phi(x_0,0)$ and $\Phi(d_2,x_f)$ are independent of the potential $U(x)$ defined on $[0,d_2]$, therefore they can be calculated separately from the design procedure of the potential $U(x)$.

The state transition matrix $\Phi(0,d_2)$ can then be computed by

$$\Phi(0,d_2) = \Phi_1 \cdots \Phi_N \tag{13}$$

where

$$\Phi_n = \Phi(x_n, x_{n+1}) = \exp\left\{-\begin{bmatrix}0 & 1\\ -K(x_n) & 0\end{bmatrix}\delta x\right\}. \tag{14}$$

Here we consider the state transition matrix from the right end $x = d_2$ to the left end $x = 0$. When $K(x_n) > 0$

$$\Phi_n = \begin{bmatrix}\cos k_n\delta x & -\sin k_n\delta x/k_n\\ k_n \sin k_n\delta x & \cos k_n\delta x\end{bmatrix} \tag{15}$$

where $k_n = \sqrt{K(x_n)}$; and when $K(x_n) < 0$

$$\Phi_n = \frac{1}{2}\begin{bmatrix}e^{k_n\delta x} + e^{-k_n\delta x} & (e^{-k_n\delta x} - e^{k_n\delta x})/k_n\\ k_n(e^{-k_n\delta x} - e^{k_n\delta x}) & e^{k_n\delta x} + e^{-k_n\delta x}\end{bmatrix} \tag{16}$$

where $k_n = \sqrt{-K(x_n)}$. Note that the state transition matrices $\Phi(x_0,0)$ and $\Phi(d_2,x_f)$ can be calculated similarly. The transmission coefficient is thus $T = 1/|p_1|^2$, where

$$p_1 = \frac{1}{2}[1 \ -i/k_0]\Phi(x_0,0)\Phi_1 \cdots \Phi_N\Phi(d_2,x_f)\begin{bmatrix}1\\ik_f\end{bmatrix}. \tag{17}$$

III. Potential Profile Design

In real physical applications, there are usually constraints on the potential profile, e.g., the potential has to lie in a particular range imposed by the physical implementation. We then formulate the profile design as the following constrained least square error minimization problem on the potential vector $U = [U_1, \ldots, U_N]^T$:

$$\begin{aligned}&\underset{U}{\text{minimize}}\ J = \sum_{j=1}^{M}\frac{1}{2}\left(T\left(V_b^j\right) - T_{\text{des}}\left(V_b^j\right)\right)^2\\ &\text{subject to}\, U_{\min} \le U_n \le U_{\max},\ n = 1, \ldots, N.\end{aligned} \tag{18}$$

Here M is the number of sampling points on the desired characteristics.

In the case when there are no constraints on the potential or the constraints are loose, we can show that both gradient descent algorithm and optimal control theory yield satisfactory results with fast convergence. Nevertheless, when the physically feasible potential is restricted to a limited set, we need to deal with a constrained optimization problem. One immediate method is to add an *ad hoc* saturation step into these algorithms. However, numerical studies reveal that this significantly slows down the optimization convergence. In what follows, we will apply sequential linear programming approach to solve the constrained potential profile design efficiently.

We first transform (18) into the following minimax problem:

$$\begin{aligned}&\underset{U}{\text{minimize}}\ \max_{j\in\{1,\ldots,M\}} J_j(U)\\ &\text{subject to}\, U_{\min} \le U_n \le U_{\max},\ n = 1, \ldots, N,\end{aligned} \tag{19}$$

$$\text{where } J_j(U) = \frac{1}{2}\left(T\left(V_b^j, U\right) - T_{\text{des}}\left(V_b^j\right)\right)^2. \tag{20}$$

The function J_j quantifies the difference between the desired and the actually achieved transmission coefficients at a specific bias voltage V_b^j, and $\max_j J_j$ is the maximum error over all the sampling points $\{V_b^j\}_{j=1}^M$. When this maximum error is minimized, we expect to achieve the desired transmission coefficients characteristics.

The minimax problem has been extensively studied in the optimization literature [10]. Here we transform the minimax problem (19) into the following equivalent form:

$$\begin{aligned}&\underset{U}{\text{minimize}}\ \gamma\\ &\text{subject to}\\ &\qquad J_1(U) \le \gamma, \ldots, J_M(U) \le \gamma,\\ &U_{\min} - U(x) \le 0, U(x) - U_{\max} \le 0.\end{aligned} \tag{21}$$

Suppose that at the kth step in the iteration, the current potential profile is U^k. We need to determine a small increment ΔU^k such that $U^{k+1} = U^k + \Delta U^k$ will bring down the cost function. By first order approximation, we have

$$J_j(U^{k+1}) \approx J_j(U^k) + \nabla_{U^k}^T J_j(U^k)\Delta U^k.$$

From the definition of J_j in (20), we have

$$\nabla_{U^k} J_j = \left(T\left(V_b^j\right) - T_{\text{des}}\left(V_b^j\right)\right)\begin{bmatrix}\dfrac{\partial T\left(V_b^j\right)}{\partial U_1} \cdots \dfrac{\partial T\left(V_b^j\right)}{\partial U_N}\end{bmatrix}^T. \tag{22}$$

From (17), we get

$$\begin{aligned}\frac{\partial T\left(V_b^j\right)}{\partial U_l} &= -2T^2\text{Re}\left(p_1^\dagger\frac{\partial p_1}{\partial U_l}\right) = -T^2\text{Re}\left(p_1^\dagger[1 \ -i/k_0]\right.\\ &\left.\times\Phi(x_0,0)\left(\Phi_1 \cdots \frac{\partial\Phi_l}{\partial U_l} \cdots \Phi_N\right)\Phi(d_2,x_f)\begin{bmatrix}1\\ik_f\end{bmatrix}\right).\end{aligned} \tag{23}$$

Recalling the expressions for Φ_l in (15) and (16), we can derive $\partial\Phi_l/\partial U_l$ explicitly: when $K(x_l) > 0$

$$\begin{aligned}\frac{\partial\Phi_l}{\partial U_l} &= \frac{\partial\Phi_l}{\partial k_l}\frac{\partial k_l}{\partial U_l} = -\frac{m}{\hbar^2 k_l}\\ &\times\begin{bmatrix}-\delta x\sin k_l\delta x & -\delta x/k_l\cos k_l\delta x + 1/k_l^2\sin k_l\delta x\\ \sin k_l\delta x + k_l\delta x\cos k_l\delta x & -\delta x\sin k_l\delta x\end{bmatrix}\end{aligned} \tag{24}$$

where $k_l = \sqrt{K(x_l)}$; and when $K(x_l) < 0$, [see (25) at the bottom of the next page] where $k_l = \sqrt{-K(x_l)}$. Combining (22)–(25), we get an analytic formula to compute the gradient $\nabla_U J$.

We then obtain a sequential linear programming algorithm as follows.

1) Choose an initial guess of the potential vector $U^0 \in [U_{\min}, U_{\max}]$.
2) At the kth step, compute $J_j(U^k)$ and $\nabla_{U^k}^T J_j(U^k)$.

3) Determine the increment ΔU^k from the following linear programming problem:

$$\begin{aligned} &\text{minimize } \gamma \\ &\text{subject to } \nabla_{U^k}^T J_1(U^k)\Delta U^k + J_1(U^k) \le \gamma, \\ &\qquad \vdots \\ &\nabla_{U^k}^T J_N(U^k)\Delta U^k + J_M(U^k) \le \gamma, \\ &U_{\min} - U^k \le \Delta U^k \le U_{\max} - U^k. \end{aligned} \tag{26}$$

4) Let $U^{k+1} = U^k + \Delta U^k$.

5) Repeat (1)–(3) until a desired convergence is reached.

The main advantage of this algorithm is that in each step of the iteration, we need only to solve a linear programming problem. This makes the algorithm converge quickly.

To test the algorithm, we consider a quadratic transmission coefficient versus bias voltage characteristics described by

$$T_{\rm des}(V_b) = 0.05V_b^2 + 0.015V_b + 0.001. \tag{27}$$

Discretize the bias voltage set as $\{V_b^j\}_{j=1}^6 = \{0, 0.05, 0.10, 0.15, 0.20, 0.25\}$. Choose $N = 50$ and $U^0 = 0.3$ V as the initial guess potential. Assume that due to the implementation restrictions, the potential has to lie in the range of [0, 0.3] V. With these settings, after 100 iterations, we obtain a potential profile as shown in Fig. 2(A). The achieved transmission coefficients are plotted in Fig. 2(B). The performance of this potential profile is measured by the root mean square (RMS) and peak error (PE) indices

$$\text{RMS} = \sqrt{\frac{1}{M_1}\sum_{j=1}^{M_1}\left(\frac{T_{\rm des}\left(V_b^j\right) - T\left(V_b^j\right)}{T_{\rm des}\left(V_b^j\right)}\right)^2} = 1.44\%,$$

$$\text{PE} = \max_j \left|\frac{T_{\rm des}\left(V_b^j\right) - T\left(V_b^j\right)}{T_{\rm des}\left(V_b^j\right)}\right| = 2.90\%.$$

Here RMS quantifies the average relative error, and PE the maximum relative error. Note that the errors are calculated based on a finer grid of the bias voltage range [0, 0.25] V than the one used for optimization, as illustrated in Fig. 2(B).

Next consider a linear transmission coefficient vs. bias voltage characteristics described by

$$T_{\rm des}(V_b) = 0.1V_b + 0.005. \tag{28}$$

The resulting potential profile and achieved transmission coefficients are shown in Fig. 3, and the errors are

$$\text{RMS} = 1.86\%, \quad \text{PE} = 5.38\%.$$

These two examples demonstrate that the sequential linear programming algorithm developed here can efficiently solve the potential design with bound constraints.

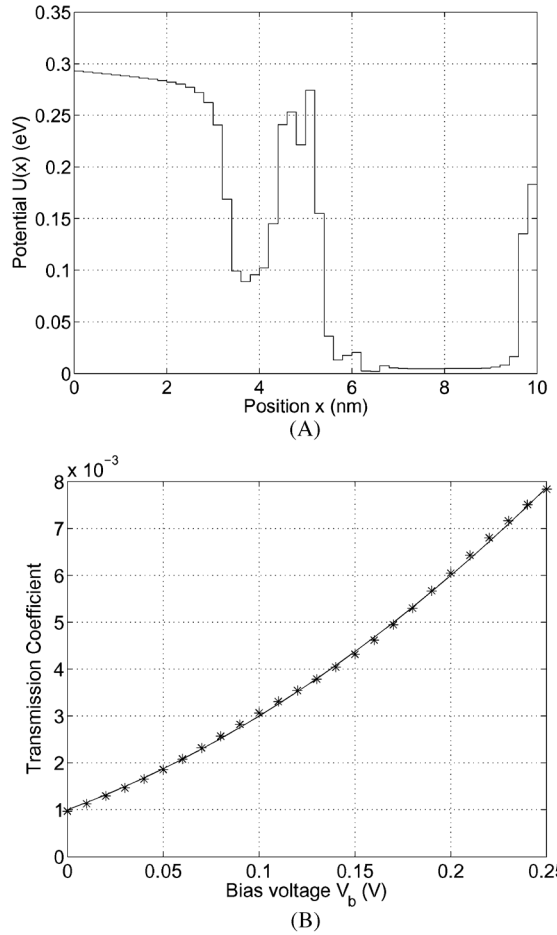

Fig. 2. Potential design result from sequential linear programming. (A) A bounded potential profile that achieves the quadratic characteristics (27) with $N = 50$; (B) solid line: desired quadratic transmission-voltage curve; star: actual transmission coefficients achieved.

IV. Robust Optimal Potential Design

Due to various imperfections, there exist noise, disturbance, and parameter uncertainty in the practical implementation of the potential. In this section, we will use robust optimization techniques to design potential that is tolerant to random disturbances.

Assume that there is a small random vector w that disturbs a certain set of parameters, which satisfies $Ew = 0$ and $Eww^T = \delta^2 I$. We want to find a potential U that solves the following optimization problem:

$$\begin{aligned} &\underset{U}{\text{minimize}} \quad E_w \sum_{j=1}^{M} \frac{1}{2}\left[\frac{T_{\rm des}\left(V_b^j\right) - T\left(V_b^j, U, w\right)}{T_{\rm des}\left(V_b^j\right)}\right]^2, \\ &\text{subject to } U_{\min} \le U_n \le U_{\max}, \quad n = 1, \ldots, N. \end{aligned} \tag{29}$$

$$\frac{\partial \Phi_l}{\partial U_l} = \frac{m}{2\hbar^2 k_l}\begin{bmatrix} (e^{k_l\delta x} - e^{-k_l\delta x})\delta x & -\left(\delta x/k_l + 1/k_l^2\right)e^{-k_l\delta x} - \left(\delta x/k_l - 1/k_l^2\right)e^{k_l\delta x} \\ (1-k_l\delta x)e^{-k_l\delta x} - (1+k_l\delta x)e^{k_l\delta x} & (e^{k_l\delta x} - e^{-k_l\delta x})\delta x \end{bmatrix} \tag{25}$$

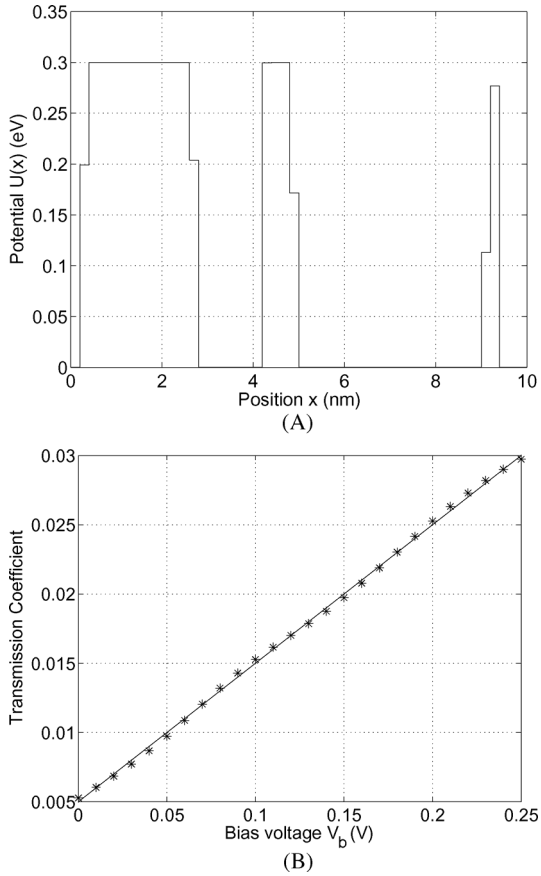

Fig. 3. Potential design result from sequential linear programming. (A) A bounded potential profile that achieves the linear characteristics (28) with $N = 50$; (B) solid line: desired linear transmission-voltage curve; star: actual transmission coefficients achieved.

The cost function is the relative error between the desired and the achieved transmission coefficients.

The optimization problem (29) is not convex and thus known robust (stochastic or worst-case) convex optimization methods [10] cannot be applied directly to find a global solution. However, they can be useful in finding a local solution. To this end, we replace the expectation E_w by an average over random samplings of the uncertain parameters drawn from their assumed known distributions. Consider a set of samples $\{w_n\}_{n=1}^{L}$. The cost function is then

$$\hat{J}(U) = \frac{1}{L}\sum_{n=1}^{L}\sum_{j=1}^{M}\frac{1}{2}\left[\frac{T_{\rm des}\left(V_b^j\right) - T\left(V_b^j, U, w_n\right)}{T_{\rm des}\left(V_b^j\right)}\right]^2.$$

Suppose that at the kth step in the iteration, we have the current potential profile U^k, and we need to determine a small increment ΔU^k so that the next potential $U^{k+1} = U^k + \Delta U^k$ will further reduce the cost function. By first order approximation, we have

$$T\left(V_b^j, U^{k+1}, w_n\right) \approx T\left(V_b^j, U^k, w_n\right) + \nabla_U^T T\left(V_b^j, U^k, w_n\right)\Delta U^k.$$

Therefore

$$\hat{J}(\Delta U^k) = \frac{1}{2}(\Delta U^k)^T\left[\sum_{n=1}^{L}\sum_{j=1}^{M}\frac{\nabla_U T\left(V_b^j, U^k, w_n\right)}{LT_{\rm des}^2\left(V_b^j\right)}\right.$$
$$\left.\times\nabla_U^T T\left(V_b^j, U^k, w_n\right)\right]\Delta U^k$$
$$+\sum_{n=1}^{L}\sum_{j=1}^{M}\frac{T_{\rm des}\left(V_b^j\right) - T\left(V_b^j, U^k, w_n\right)}{LT_{\rm des}^2\left(V_b^j\right)}$$
$$\times\nabla_U^T T\left(V_b^j, U^k, w_n\right)\Delta U^k$$
$$+\sum_{n=1}^{L}\sum_{j=1}^{M}\frac{1}{2L}\left[\frac{T_{\rm des}\left(V_b^j\right) - T\left(V_b^j, U^k, w_n\right)}{T_{\rm des}\left(V_b^j\right)}\right]^2.$$

Now the cost function $\hat{J}(\Delta U^k)$ is quadratic in ΔU^k, and it can be solved quickly and reliably by quadratic programming. We thus obtain a local solution to (29) by using the following iterative algorithm.

1) Take an initial guess of potential $U^0 \in [U_{\min}, U_{\max}]$;

2) At the kth step, for all j and n, compute $T(V_b^j, U^k, w_n)$ and $\nabla_U T(V_b^j, U^k, w_n)$, and let

$$A^k = \sum_{n=1}^{L}\sum_{j=1}^{M}\frac{\nabla_U T\left(V_b^j, U^k, w_n\right)\nabla_U^T T\left(V_b^j, U^k, w_n\right)}{LT_{des}^2\left(V_b^j\right)}$$

and

$$b^k = \sum_{n=1}^{L}\sum_{j=1}^{M}\frac{T_{des}\left(V_b^j\right) - T\left(V_b^j, U^k, w_n\right)}{LT_{des}^2\left(V_b^j\right)}\nabla_U T(V_b^j, U^k, w_n);$$

3) Determine an increment ΔU^k by solving the following quadratic programming problem

$$\underset{\Delta U^k}{\text{minimize}}\ \frac{1}{2}(\Delta U^k)^T A^k \Delta U^k + (b^k)^T \Delta U^k$$
$$\text{subject to}\ U_{\min} - U^k \le \Delta U^k \le U_{\max} - U^k;$$

4) Let $U^{k+1} = U^k + \Delta U^k$;

5) Repeat (1)–(3) until a desired convergence is reached.

We apply this algorithm to an example. Assume that there exist small errors in determining the dielectric constants for the materials, i.e., instead of the nominal value $\epsilon_1 = 13.1\epsilon_0$ and $\epsilon_2 = 10.6\epsilon_0$, we have

$$\epsilon_1 = 13.1(1 + w_1)\epsilon_0 \qquad \epsilon_2 = 10.6(1 + w_2)\epsilon_0.$$

Here w_1 and w_2 are both small random variables. These parameter discrepancies between the model and the process affect the conduction band potential in (2) and in turn alter the transmission coefficients. We want to design a potential profile that achieves the linear transmission coefficient versus bias voltage relation in (28)

$$T_{\rm des}(V_b) = 0.1V_b + 0.005$$

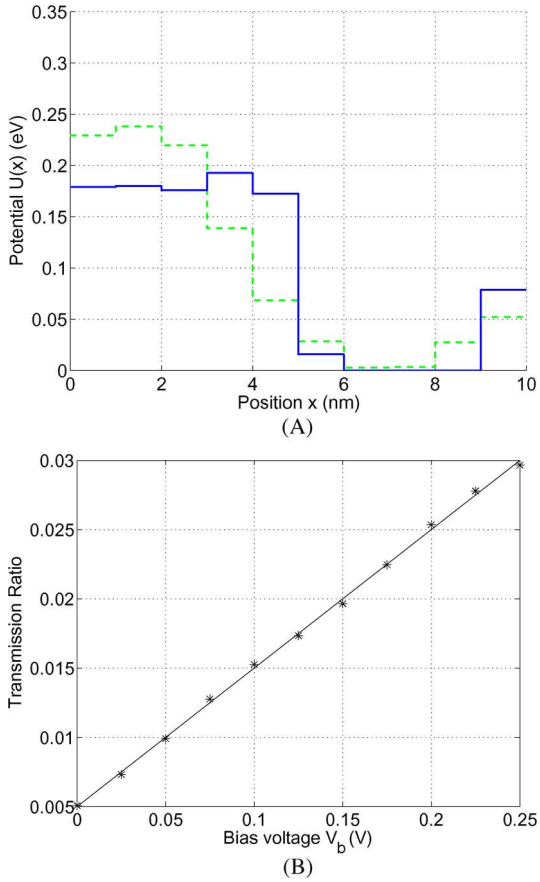

Fig. 4. Robust potential design results. (A) Green dashed line: initial potential obtained from sequential linear programming with $N = 10$ and RMS 1.88%; Blue solid line: potential from robust design with RMS 1.49%; (B) solid line: desired linear transmission-voltage curve; star: actual transmission coefficients achieved by the robust potential design.

and at the same time is robust against parameter uncertainty in material dielectric constants.

First assume that both w_1 and w_2 are random variables uniformly distributed in the range $[-0.01, 0.01]$, i.e., they represent a 1% level of relative parameter uncertainty. For both w_1 and w_2 we generate a set of 100 independently drawn samples. Hence $L = 100$. Our starting potential profile, shown by green dashed line in Fig. 4(A), is obtained from the sequential linear programming in Section III, and it has an RMS error of 1.88%. After applying the robust optimization algorithm with 200 iterations, we obtain a potential shown as blue solid line in Fig. 4(A). For no uncertainty this potential has an RMS error of 1.49%, and its transmission-voltage curve is shown in Fig. 4(B). Surprisingly the RMS error of the robust potential is smaller than that of the initial potential. The reason for this is that there are many suboptimal solutions with similar nominal values, but not all of them are equally robust.

To demonstrate that the resulting potential profile is indeed more robust against the uncertainty in dielectric constants than the initial potential, we calculate the RMS errors of achieved transmission coefficients for a set of 1000 samples for both potentials. In Fig. 5, the top plot shows the histogram distribution of RMS errors for the initial potential and the bottom plot for the robust potential. The dashed line indicates the 90th percentile. It is evident that the robust potential reduces the RMS error when dielectric constants are not precisely known.

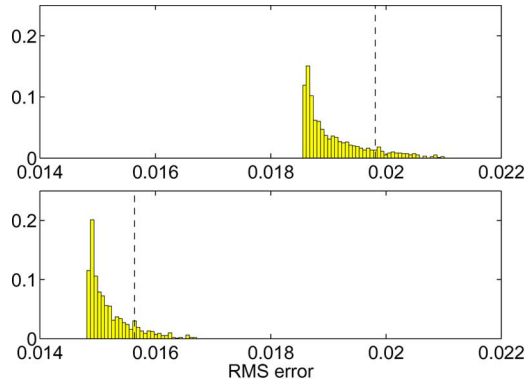

Fig. 5. Histogram distributions of RMS errors for (top) initial potential and (bottom) robust potential. Dashed line: 90th percentile.

V. Conclusion

In this brief we discussed the design of potential profile to achieve a desired electron transmission characteristics in nanoscale semiconductor devices. We formulated it as a constrained minimization problem, and applied sequential linear programming to solve it. We also studied the robust potential design that provides a consistent transmission characteristics when there are possible noise, disturbance, and parameter uncertainty in the device.

Transmission coefficients characteristics is our first attempt to apply optimization techniques to solve design problems in nanoscale semiconductor devices. We plan to extend this study to investigate more challenging problems such as resonant tunneling in the future.

Acknowledgment

The authors would like to thank the anonymous referees for their in-depth revising comments.

References

[1] *Single Quantum Dots: Fundamentals, Applications, and New Concepts*, P. Michler, Ed.. Berlin, Germany: Springer-Verlag, 2010.
[2] O. J. Glembocki, *Nanoparticles and Nanowire Building Blocks—Synthesis, Processing, Characterization and Theory*. San Francisco, CA: Materials Research Society, Apr. 2004.
[3] D. K. Schroder, *Semiconductor Material and Device Characterization*, 3rd ed. New York: Wiley-IEEE Press, 2006.
[4] S. Martinie, D. Munteanu, G. Le Carval, and J.-L. Autran, "Physics-based analytical modeling of quasi-ballistic transport in double-gate MOSFETs: From device to circuit operation," *IEEE Trans. Electron Devices*, vol. 56, no. 11, pp. 2692–2702, Nov. 2009.
[5] P. Schmidt, S. Haas, and A. F. J. Levi, "Synthesis of electron transmission in nanoscale semiconductor devices," *Appl. Phys. Lett.*, vol. 88, p. 013502, 2006.
[6] A. F. J. Levi and I. G. Rosen, "A novel formulation of the adjoint method in the optimal design of quantum electronic devices," *SIAM Jo. Control Opt.*, vol. 48, no. 5, pp. 3191–3223, 2010.
[7] S. Wang, *Fundamentals of Semiconductor Theory and Device Physics*. Englewood Cliffs, NJ: Prentice-Hall, 1989.
[8] A. F. J. Levi, *Applied Quantum Mechanics*. Cambridge, U.K.: Cambridge University Press, 2002.
[9] B. H. Bransden and C. J. Joachain, *Introduction to Quantum Mechanics*. Essex, U.K.: Longman Scientific & Technical, 1989.
[10] S. Boyd and L. Vandenberghe, *Convex Optimization*. Cambridge, U.K.: Cambridge University Press, 2004.